

RESEARCH

Open Access



Unlocking the potential of β -1,3-xylooligosaccharides from *Caulerpa lentillifera*: structural characterization, antioxidative and anti-osteoarthritis applications

Lixi Cai^{1,3}, Jinlin Zheng^{1,3}, Lixing Liu^{1,3}, Xiaoping Chen^{1,3} and Honglin Wang^{2*}

Abstract

Background β -1,3-Xylooligosaccharides (XOS-3) extracted from *Caulerpa lentillifera* have shown potential antioxidative and anti-tumor properties, but research on their biological activities, particularly their anti-osteoarthritis effects, is still in early stages.

Results XOS-3 were produced by eco-friendly enzymatic hydrolysis, displaying a semi-crystalline structure with predominant xylose, xylobiose, xylotriose, and xylotetraose components which were confirmed by IC, SEM, FT-IR, and XRD analysis. Compared with β -1,4-xylooligosaccharides, XOS-3 had stronger antioxidant properties, and the scavenging rate of $O_2^{\cdot-}$ and DPPH $^{\cdot}$ radicals was 82.31% and 58.44% at 2.0 mg/mL respectively. In vitro studies, XOS-3 significantly improved cell viability in IL-1 β -induced rat chondrocytes from 43.41 to 73.5% at 100 μ g/mL, demonstrating anti-inflammatory and cartilage-protective effects by modulating MMP13 and COL2A1 expression.

Conclusions The study displayed the potential antioxidative and anti-osteoarthritis effects of XOS-3, offering new visuals for the development of marine polysaccharides in the treatment of osteoarthritis.

Keywords β -1,3-xylan, β -1,3-xylooligosaccharides, Antioxidant, Osteoarthritis, Enzymatic hydrolysis

*Correspondence:

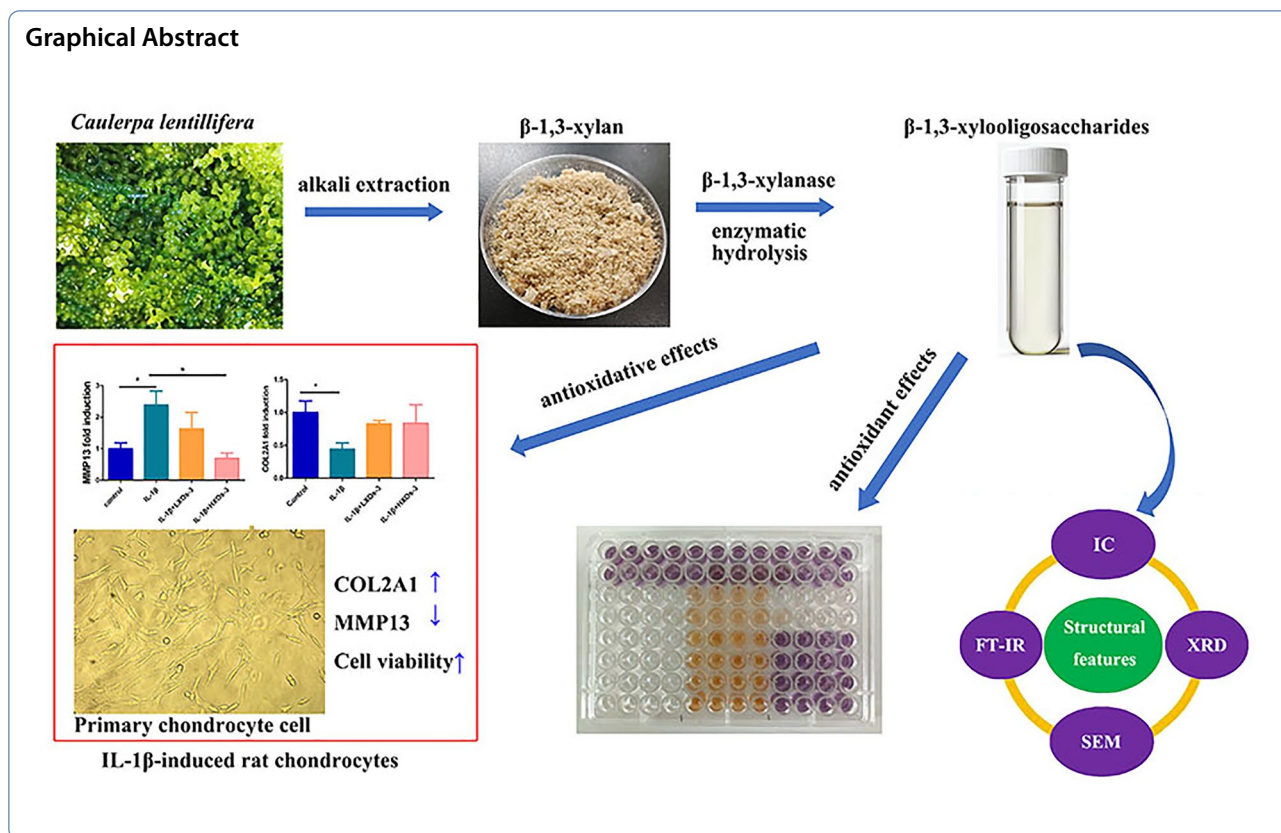
Honglin Wang

hmlovewhl@outlook.com

Full list of author information is available at the end of the article



© The Author(s) 2024. **Open Access** This article is licensed under a Creative Commons Attribution 4.0 International License, which permits use, sharing, adaptation, distribution and reproduction in any medium or format, as long as you give appropriate credit to the original author(s) and the source, provide a link to the Creative Commons licence, and indicate if changes were made. The images or other third party material in this article are included in the article's Creative Commons licence, unless indicated otherwise in a credit line to the material. If material is not included in the article's Creative Commons licence and your intended use is not permitted by statutory regulation or exceeds the permitted use, you will need to obtain permission directly from the copyright holder. To view a copy of this licence, visit <http://creativecommons.org/licenses/by/4.0/>. The Creative Commons Public Domain Dedication waiver (<http://creativecommons.org/publicdomain/zero/1.0/>) applies to the data made available in this article, unless otherwise stated in a credit line to the data.



Introduction

β -1,3-xylan, a unique polysaccharide composed of β -1,3-linked D-xylose, was found in some marine red or green algae, such as *Caulerpa*, *Bangia*, and *Porphyra* spp [1, 2]. Unlike land plants, the cell walls of these algae completely lack cellulose and mainly rely on β -1,3-xylan to maintain their mechanical strength which has not been found in land plants that contain β -1,4-xylan instead [3–5]. The high molecular weight, degree of polymerization, and poor solubility of xylan limit their biological activity across cell membranes [6]. Therefore, degrading macromolecular plant polysaccharides into smaller xylooligosaccharides (XOS) presents a significant opportunity for enhancing their biological utilization [7, 8]. However, research on the XOS production from marine biomass remains scarce [9, 10]. In this context, exploring an increasing variety of marine algae as feedstocks for XOS production is a promising avenue [11, 12]. β -1,3-xylooligosaccharides (XOS-3), the degraded products extracted from β -1,3-xylan, demonstrate notable biological activities distinct from β -1,4-xylooligosaccharides (XOs-4), attributed to their unique structural linkages [13, 14]. Liang et al. demonstrated that XOs-3 extracted from *Caulerpa lentillifera* (*C. lentillifera*) exhibited antioxidant and anticoagulant activities [15]. Maeda et al.

reported that XOs-3 extracted from *C. lentillifera* could have anti-tumor and anti-microbial therapeutic effects by enhancing the functions of macrophage RAW264.7 cells, including cell phagocytosis, NO production, cytokine induction, and regulation of host immune response [16]. Such findings provide a solid basis for future investigations into activities, mechanisms and utilization of algal XOS-3 resources.

Producing XOs-3 by β -1,3-xylanase hydrolysis is an efficient way. It neither requires any expensive equipment nor generates undesirable byproducts. These factors make it a fast and economical method which is more eco-friendly compared to physical and chemical hydrolyses [17–19]. However, only a few scholars in Japan, Taiwan, and China have begun to study β -1,3-xylanase, and only nine β -1,3-xylanases have been found and verified [20–22]. Thus, the information on XOS-3 and their potential biological activities is scarce, and the study on the XOS-3 from *C. lentillifera* and their biological activities is of great significance.

Osteoarthritis (OA) is a progressive degenerative joint disease that affects nearly half of the elderly population, posing enormous pressure on healthcare systems and society as a whole [23–25]. The pathological changes of OA are closely associated with cellular aging, chronic

inflammation, and matrix degradation in joint tissues, which may be caused by mitochondrial dysfunction and oxidative stress [26, 27]. Therefore, mitigating oxidative stress-induced chondrocytes damage emerges as a promising strategy for OA treatment. Previous research has explored the potential applications of various types of XOS in OA treatment, including those derived from sucrose, chitosan, acetylated chitin, glycosaminoglycans, chondroitin sulfate E, and hyaluronic acid, offering good insights into a range of therapeutic mechanisms and outcomes [28–33]. Currently, XOS-3 has demonstrated anti-oxidative, antitumor, and anti-inflammatory properties [16, 18]. However, its specific potential and application in OA treatment remain unexplored. Given this, we first prepared β -1,3-xylan from *C. lentillifera*, and used β -1,3-xylanase (Xyl3088) with the highest activity isolated and reported by our laboratory, to hydrolyze and control its degree of hydrolysis [2, 34]. This study not only verifies the advantages of XOS-3 in reducing oxidative stress but also aims to elucidate the protective mechanisms of XOS-3 on chondrocytes. It provides a scientific basis for using XOS-3 in OA treatment and aim to discover the significant active components in XOS-3, which will provide a theoretical basis for the deep product development, and utilization of biological seaweed resources.

Materials and methods

Polysaccharide isolation

β -1,3-xylan was prepared from *C. lentillifera* (Nhatrang, Vietnam) by adopting the laboratory-modified method of Iriki et al. [35]. Briefly, *C. lentillifera* were washed, dried and ground into a powder that can pass 200 mesh screens. The resulting powder (20 g) was treated successively with NaOH (0.3 mol/L, 1 L) and H₂SO₄ (0.25 mol/L, 1 L) with stirring for 30 min at 100 °C respectively. The precipitate was bleached with NaClO₄ (1%, 1 L) for 2 h at 25 °C, and re-suspended in ddH₂O. NaOH (2.5 mol/L, 0.8 L) was added to the bleached residue treated in the ice bath for 3 h, and the extracted polysaccharide was then mixed with four volumes of ethanol and left to precipitate overnight at 4 °C. The precipitated β -1, 3-xylan was neutralized with 5.7 mol/L acetic acid followed by washing with ddH₂O, and finally freeze-dried overnight. The total concentration of polysaccharides was quantified by the phenol sulfuric acid method with D-xylose as the standard [34].

Preparation of XOS

Xyl3088 (GenBank accession No. MK253053), derived from *Flammeovirga pacifica* strain WPAGA1, was expressed in *Escherichia coli* L21(DE3) cells. The expression was induced by loading 0.5 mmol/L IPTG, followed by incubation at 18 °C, and 180 rpm for 16 h. The cells

were collected and lysed via sonication at 300 W for 20 min on ice. The resulting lysate was then centrifuged at 12,000×g for 20 min to remove the insoluble cell debris. The supernatant which containing the crude Xyl3088 was filtered through 0.45 μ m sterilized filters before being loaded onto a nickel affinity column (1.4×6.5 cm, Smart-Lifesciences, China) for purification. Elution of proteins were performed using an elution buffer composed of 50 mmol/L Tris-Cl, 500 mmol/L NaCl, and imidazole concentrations of either 250 mmol/L or 80 mmol/L, respectively.

β -1,3-xylan (1%, w/v) or β -1,4-xylan (Macklin, X823251, 1%, w/v) were incubated with β -1,3-xylanase or β -1,4-xylanase in a total volume of 2 mL at 37 °C for 24 h. Then enzymes were inactivated by heating at 100 °C for 5 min. To detect the enzymatic hydrolysis product, 3,5-dinitrosalicylic acid (DNS) was loaded into the reaction liquid and heated at 100 °C for 5 min, then centrifuged at 12,000×g for 5 min. The supernatant was taken for assay at 540 nm using D-glucose as the standard for total reducing sugar.

XOS-3 prepared by trifluoroacetic acid (TFA) method was performed as follows: β -1,3-xylan (1 g) was incubated with TFA (1 mol/L, 20 mL) at 70 °C for 3 h. The supernatant was taken by centrifugation at 25 °C (12,000×g, 10 min) to remove the residual insoluble β -1,3-xylan and then was neutralized with NaOH (1 mol/L).

Ion chromatography

The XOS-3 were identified by ion chromatography (IC; Dionex ICS3000, American) equipped with a Dionex CarboPacPA-100 (4 mm×250 mm). Eluent was separated at a flow rate of 0.3 mL/min using different gradients of 100 mmol/L NaOH (200 mM NaOAc) with the column temperature maintained at 30 °C, the pump and the sample amount was 20 μ L [21].

Characterization of XOS

The morphology and size of XOS-3 were detected by scanning electron microscopy (SEM, HITACHI, SU8010). The elementary composition of XOS-3 was characterized by energy-dispersive X-ray spectrometry (EDS). Then, the Fourier transform infrared spectroscopy (FT-IR, Nexus-870) of XOS-3 was obtained in the range of 4000 cm⁻¹ to 400 cm⁻¹. Finally, X-ray diffraction (XRD) patterns were performed at 40 kV and 15 mA using a Tongda TD-3500 X-ray diffractometer to analyze the average particle size of XOS-3.

Free radicals scavenging activity

XOS-3 and XOS-4 were prepared at final concentrations of 0.1, 0.2, 0.5, 1.0, 1.5 and 2.0 mg/mL, respectively. The antioxidant activities of samples were evaluated by

2-diphenyl-1-pyridyl hydrazine (DPPH[•]), hydroxyl (OH[•]), superoxide (O₂^{•-}), and 2,2'-azino-bis(3-ethylbenzothiazoline-6-sulfonate) (ABTS^{•+}) radical scavenging ability respectively, Vitamin C (Vc) was the positive control group. The test method was described by Ji et al. [36].

The reducing abilities of the XOS-3 and XOS-4 were performed as follows: 2.5 mL of XOS-3 and XOS-4 (0.1, 0.2, 0.5, 1, 1.5, 2.0 mg/mL) were cultured with 2.5 mL Tris-HCl (pH 7.0) and 2.5 mL K₃Fe(CN)₆ (1%) at 50 °C for 20 min and then 0.5 mL trichloroacetic acid (10%) was loaded into the mixture, followed by centrifugation at 3000×g for 10 min, 5 mL supernatant was taken with 0.1 mL FeCl₃ and 5 mL ddH₂O for assay at 700 nm. Vc was the positive control group.

$$\text{Fe}^{2+} \text{ radical scavenging activity (\%)} \\ = \left[1 - \frac{A_x - A_{x0}}{A_0} \right] \times 100\%$$

where A_x was the absorbance of the sample reaction mixture, A_{x0} was the absorbance of the sample color removal group, A_0 was the absorbance of the reaction mixture replacing the sample solution with ddH₂O.

Culture of primary articular chondrocyte cell

Primary articular chondrocytes were isolated from the femoral heads, femoral condyles, and tibial plateau of 10-day-old Wistar rats (purchased from Wusi Laboratory Animal Co., Ltd.). After the cartilage was digested with trypsin (0.25%; Hyclone) at 37 °C for 30 min and collagenase II (0.2%; Sigma-Aldrich) at 37 °C for 4 h, the primary chondrocytes were resuspended and cultured in dulbecco's modified eagle medium/nutrient mixture F-12 (DMEM/F12; Hyclone) supplemented with 1% streptomycin-penicillin (Hyclone) and 10% fetal bovine serum (Gibco, Australia) at 37 °C under 5% CO₂ atmosphere. Chondrocytes in the second passage were used in our study. Chondrocytes were stained with toluidine blue (Solarbio) according to the manufacturer's instructions.

Cell viability assays

The cell counting kit-8 (CCK8, Beyotime) assay was applied to test the cellular viability. Chondrocytes were plated into 96-well plates at a density of 1,0000 cells per well and cultured with IL-1β (10 ng /mL) to induce cell death in OA. XOS-3 (0, 0.05, 0.1 mg/mL) were applied to rescue chondrocyte death. Then, 10 μL of CCK8 solution was loaded to each well after 24 h to detect the absorbance at a wavelength of 450 nm by the microplate spectrophotometer (Mode ELx800, Biotek, USA) after another 2 h culture at 37 °C.

Western blot analysis

Chondrocytes were lysed with 100 μL radio immunoprecipitation assay lysis buffer (Beyotime, China) that contained a 1% proteinase inhibitor cocktail and separated by 12% SDS polyacrylamide gel electrophoresis (SDS-PAGE). After transferring to the polyvinylidene fluoride membranes (PVDF), the membranes were incubated with primary antibodies overnight at 4 °C and with secondary antibodies for another 2 h at room temperature. Protein bands were visualized using a Bio-Rad ChemiDoc XRS+ system. Proteins were analyzed with antibodies recognizing MMP13 (1:2000, Proteintech Cat# 18165-1-AP), COL2A1 (1:1000, Immunoway Cat# YT-1022), GAPDH (1:1000, Immunoway # YM-3029).

Statistical analysis

SPSS 27 was applied for all statistical analyses. Data from multiple experiments were expressed as mean ± S.E.M and compared by one-way ANOVA multiple comparisons test. All experiments were performed independently at least 3 times.

Results and discussion

β-1, 3-xylan isolation

The extraction rate of β-1,3-xylan from *C. lentillifera* was 13.45% ± 0.67% by alkali extraction which was suitable for large-scale production. Zhang et al. employed water extraction, alcohol precipitation, and ultrasonic-assisted extraction methods to extract the polysaccharide from *C. lentillifera* with ddH₂O as extracting solvent for 9.07 h at 100 °C with 1:40 g·mL⁻¹ of the solid-liquid ratio [37]. However, the final yield was only 3.22%. In contrast, the yield from alkali extraction was 4.18 folds that of water extraction, making it ideal for mass production.

XOS generation and characterization

β-1,3-xylanase (Xyl3088), with the highest activity isolated and reported by Zhang et al., was used to hydrolyze β-1,3-xylan and control the degree of hydrolysis of XOS-3 [20]. This hydrolysis process stood as the most environmentally friendly alternative for producing XOS-3, not requiring any special equipment (low temperatures and pressure) or strong chemical compounds [38]. It also doesn't create any unwanted byproducts. Compared to physical and chemical hydrolyses, it's quicker and better for the environment, displaying an alternative strategy for generating the bioactive compounds such as XOS from renewable resources [39, 40].

The composition of XOS-3, degraded by enzyme and trifluoroacetic acid was qualitatively detected by

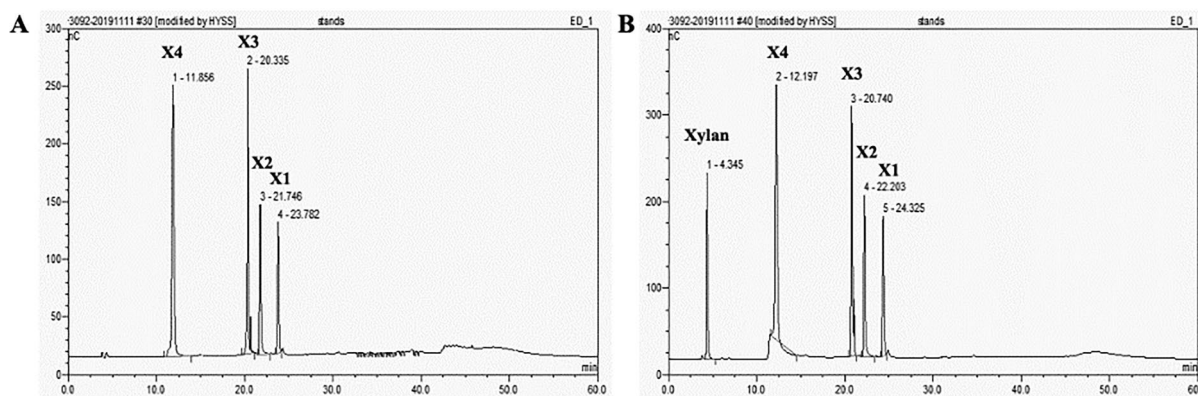


Fig. 1 Ion chromatography analysis of the product profiles: **A** Prepared by trifluoroacetic acid; **B** Prepared by β -1,3-xylanase

ion chromatography. As shown in Fig. 1A and B, two hydrolysis products consisted of similar compositions of XOS-3: xylose (X1), xylobiose (X2), xylotriose (X3), and xylotetraose (X4), with X3 and X4 being the most abundant. These results were consistent with the IC results of XOS-3 composition of Cai et al. [21]. Unlike the enzymatic hydrolysis products, xylan was not or little detected in the products of trifluoroacetic acid (Fig. 1A). It was speculated that the differences in the composition of XOS-3 between enzymatic and acid hydrolysis were due to the more intense reaction conditions and the more thorough reaction of xylan by trifluoroacetic acid.

The surface morphologies and microstructures of XOS-3 were analyzed by SEM. Figure 2A and B demonstrated that XOS-3 was relatively smooth with irregular blocklike structures. It might be due to oligosaccharides with high molecular weight being more likely to form hydrogen bonds between oligosaccharides [36, 41], therefore, XOS-3 showed a relatively aggregate state.

The functional groups and chemical bonds of XOS-3 were detected by FT-IR spectrum (Fig. 2C). The O–H and C–H stretching vibrations were demonstrated by absorption peaks at 3423 and 2921 cm^{-1} , respectively. The peak at 1743 cm^{-1} indicated the presence of uronic acid, while the peak at 1631 cm^{-1} suggested symmetrical C=O-stretching vibrations [42]. Peaks at 1411 cm^{-1} and 1041 cm^{-1} indicated the typical absorption of C–H bands and the pyranose form's C–O–stretching vibrations, respectively. The weak characteristic peaks appearing at 800–900 cm^{-1} may indicate the presence of α - and β - configuration [43]. In short, FT-IR analysis confirmed that XOS-3 exhibits typical absorption peaks of oligosaccharides.

XRD analysis was commonly used to evaluate the crystallinity of polysaccharides and XOS. The diffraction intensity curve of XOS-3 within the range of 5–80° shown sharp and narrow peaks at 2θ of 26°, 31°, 45°,

55° and 75° (Fig. 2D), indicating that XOS-3 tends to be semi-crystalline.

Antioxidant effects of XOS

The accumulation of free radicals typically increases during both acute and chronic diseases in humans [44]. Some XOS have been reported to protect the body from oxidative damage, suggesting potential biomedical applications. Hydroxyl radical (OH^{\bullet}), the most reactive and toxic of all free radicals, can damage DNA and even lead to cell mutation and death. As shown in Fig. 3A, both Vc and XOS-3 reduced the colored substances until they disappeared; the yellow color in XOS-3 was due to the original color of XOS-3, while the removal ability of XOS-4 for OH^{\bullet} was very low, and the colored substance did not disappear. At the concentration of 1.5 mg/mL, the scavenging rate of XOS-3 reached 98.13%, almost identical to that of Vc (98.65%), while the removal rate of XOS-4 was only 7.44% (Fig. 3B). The results indicated that the scavenging activities of XOS-3 on OH^{\bullet} radicals were significantly higher than that of XOS-4.

DPPH $^{\bullet}$ radical has been used as a classical model for determining the antioxidative activity in vitro of XOS. The scavenging activities of Vc and XOS-3 on DPPH $^{\bullet}$ radical were in a dose-dependent manner (Fig. 3C). The scavenge rates of Vc and XOS-3 were 62.83% and 58.44% at a concentration of 2 mg/mL respectively, higher than that of XOS-4 (20.36%).

ABTS $^{+\bullet}$ radicals were also frequently used to evaluate antioxidant capability. As shown in Fig. 3D, the ABTS $^{+\bullet}$ radicals scavenging activities of XOS-3 (96.18%) and Vc (100.30%) were more potent than that of XOS-4 (29.73%) at 0.5 mg/mL, indicating that XOS-3 was an effective scavenger for ABTS $^{+\bullet}$ radicals.

$\text{O}_2^{\bullet-}$ radical is one of the precursors of singlet oxygen and hydroxyl radicals with a strong oxidation capacity. As shown in Fig. 3E, XOS-3 and Vc exhibited significant

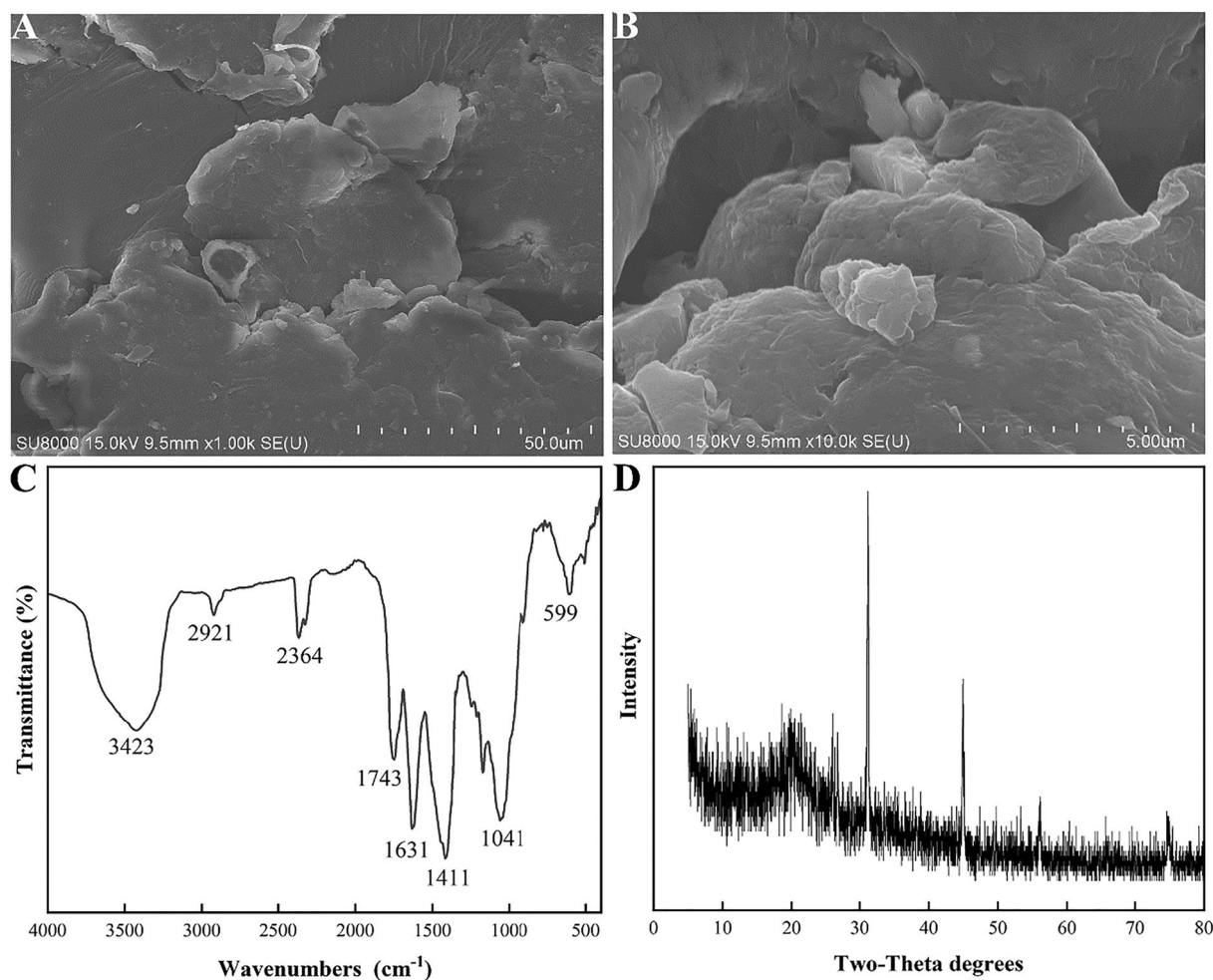


Fig. 2 The physicochemical analysis of XOS-3: **A** Scanning electron microscopy $\times 1000$; **B** Scanning electron microscopy $\times 10000$; **C** FT-IR spectrum; **D** X-ray diffraction pattern

scavenging activities for $O_2^{\cdot-}$ radicals in a dose-dependent manner. The scavenging ability of XOS-3 (82.31%) was slightly lower than that of Vc (97.32%), but much stronger than that of XOS-4 (39.83%) at 2.0 mg/mL. Although the scavenging capacity of XOS-3 was slightly lower than Vc, it is still considered as an effective electron donor adjuvant due to its low side effects and toxicity.

The Fe^{2+} chelating has been widely used in antioxidant tests for XOS [45]. Figure 3F showed that the Fe^{2+} chelating activities of Vc, XOS-3, and XOS-4 all gradually increased as the sample concentration increased. The scavenging ability of XOS-3 (68.92%) was lower than that of Vc (86.24%), but significantly higher than that of XOS-4 (11.33%) at a concentration of 2.0 mg/mL, indicating XOS-3 had a certain reduction energy.

The superior antioxidant capacity of XOS-3 compared to XOS-4 is attributed to differences in production methods, substrate origins, degrees of polymerization and molecular structures. Valls et al. found that XOS derived from glucuronoxylan by different xylanases exhibited varied antioxidant activities [46]. Xue et al. demonstrated that the antioxidant activity of XOS was affected by the sources of xylan and the degree of polymerization, especially some extracts from algae displayed superior antioxidant activities [47]. Ji and Yuan revealed that the position and type of glycosidic bond would influence biological activity of polysaccharides or XOS, and shown that (1 \rightarrow 3) glycosidic bonds played an important role in enhancing anti-inflammatory effects and immune

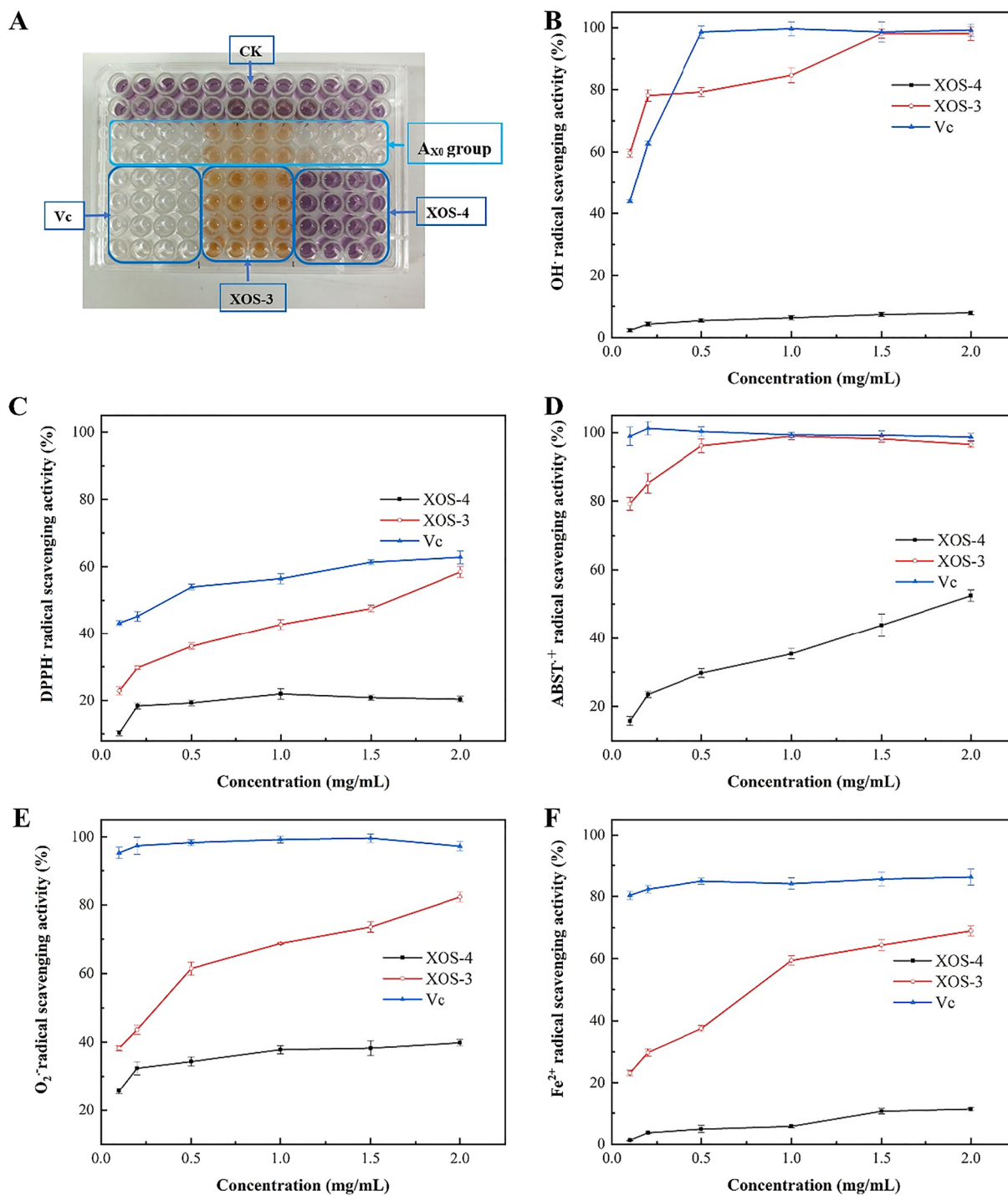


Fig. 3 Antioxidant activity of XOS-3, XOS-4, and Vc: **A** Effect diagram of scavenging activity of $\text{OH}\cdot$; **B** The scavenging activity of $\text{OH}\cdot$ radical; **C** The scavenging activity of $\text{DPPH}\cdot$ radical; **D** The scavenging activity of $\text{ABTS}\cdot^+$ radical; **E** The scavenging activity of $\text{O}_2\cdot^-$ radical; **F** The chelating activity of Fe^{2+}

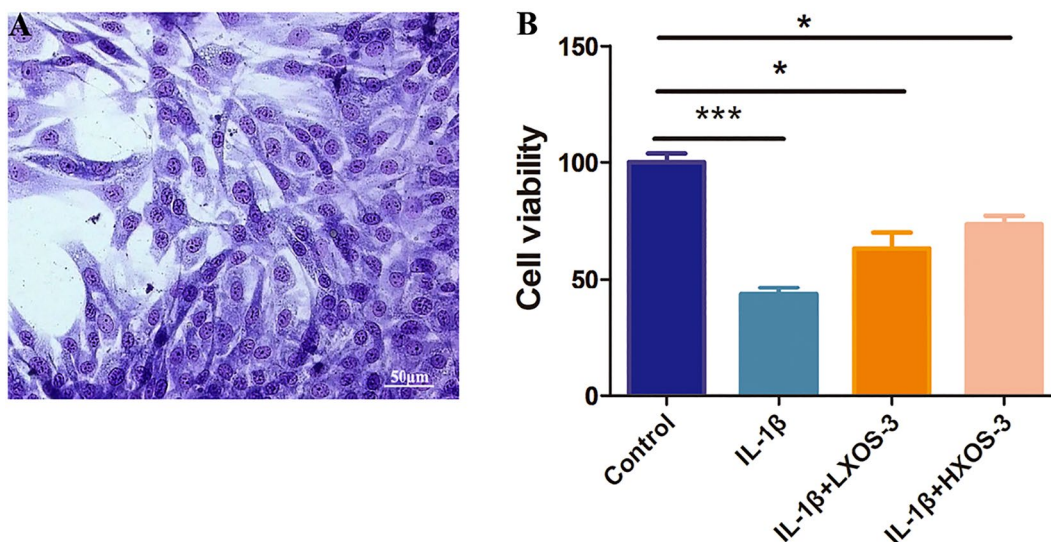


Fig. 4 Primary articular chondrocyte cells and their cell viability: **A** Toluidine blue staining of primary articular chondrocyte cells. **B** Effect of XOS-3 on IL-1 β -induced chondrocyte proliferation. Data were presented as the mean \pm SD; * p < 0.05, *** p < 0.001

regulation [48, 49]. Consequently, a comprehensive study of the structural characteristics of XOS-3 and its antioxidant mechanisms should be performed for

elucidating the structure-bioactivity relationship and identifying high-potential antioxidants.

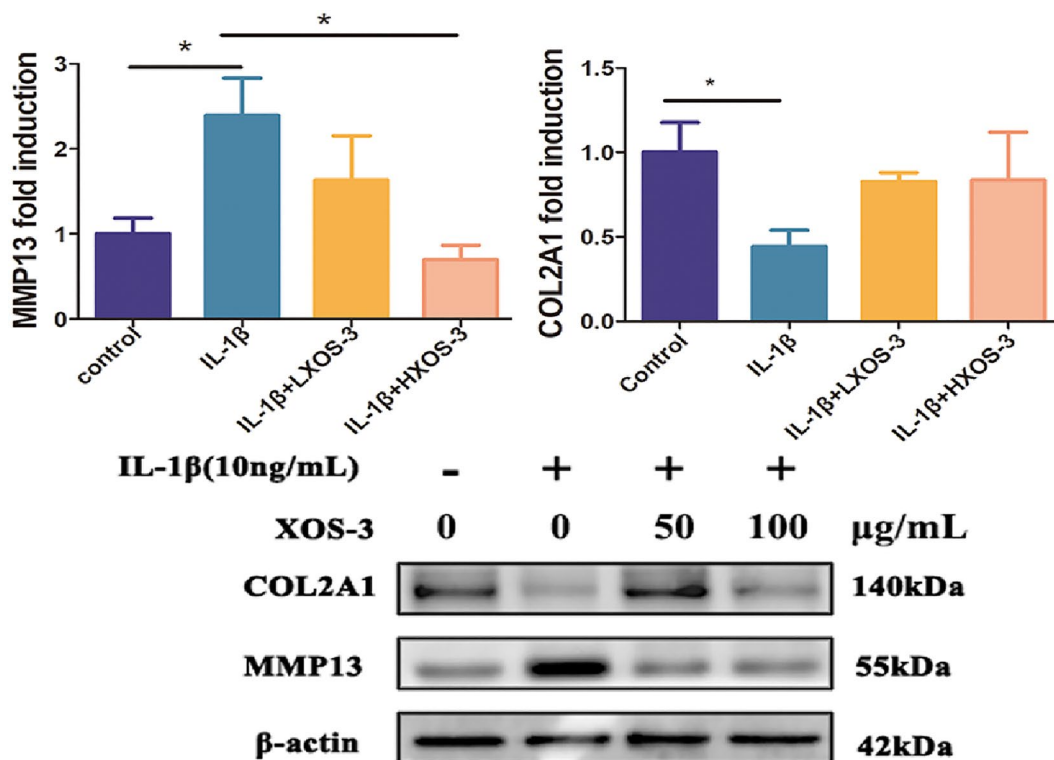


Fig. 5 Immunoblotting results of MMP13 and COL2A1, and the quantification of MMP13 and COL2A1, with β -actin as the endogenous control. Data were presented as the mean \pm SD; * p < 0.05

Anti-osteoarthritis activity

To assess the anti-inflammatory effects of XOS-3, primary articular chondrocyte cells were chosen for anti-osteoarthritis studies. Toluidine blue staining revealed that chondrocyte cells were triangular or polygonal with purplish-blue nuclei and light purplish-blue cytoplasm (Fig. 4A). The cells were consistent with the characteristics of chondrocytes and suitable for subsequent experiments.

To simulate the inflammatory environment of osteoarthritis in vitro, rat chondrocytes were induced with 10 ng/ml IL-1 β . As shown in Fig. 4B, the cell viability of simulated chondrocytes significantly decreased to 43.41% ($p < 0.001$), while after treatment with LXOS-3 (50 μ g/mL) and HXOS-3 (100 μ g/mL), the cell viability of chondrocytes increased to a significant level at 63.22% ($p < 0.05$) and 73.5% ($p < 0.05$), respectively.

The cartilage anabolic factor COL2A1 and the catabolic factor MMP13 were critical for maintaining articular cartilage homeostasis. To evaluate the role of XOS-3 in anti-osteoarthritis function, the expression levels of MMP13 and COL2A1 were investigated using Western blot analysis (Fig. 5). The MMP13 level in IL-1 β -stimulated chondrocytes markedly increased to 2.39 compared to the control group ($p < 0.05$), which decreased to 1.63 with LXOS-3 treatment and 0.70 with HXOS-3 treatment respectively. The COL2A1 level was significantly reduced to 0.44 ($p < 0.05$), which increased to 0.83 with LXOS-3 treatment and 0.84 with HXOS-3 treatment. XOS-3 may inhibit the progression of OA through several mechanisms. Firstly, the antioxidant properties of XOS-3 may directly neutralize ROS, thereby reducing oxidative stress and promoting the expression of COL2A1 [50, 51]. Furthermore, XOS-3 can mitigate inflammation by reducing the production of inflammatory cytokines. This reduction may lead to the downregulation of MMP13, thereby reducing cartilage degradation and enhancing the repair or maintenance of cartilage tissue. Overall, these findings indicated that XOS-3 potentially slowed down the degeneration of cartilage during OA progression, highlighting the therapeutic potential of XOS-3 in treating oxidative stress-related diseases and osteoarthritis [52].

Conclusions

A novel approach for the production of XOS-3 by eco-friendly enzymatic hydrolysis was tailored, marking a major advance in the sustainable extraction of marine polysaccharides. The detailed structural characterizations by IC, SEM, FT-IR, and XRD have revealed the semi-crystalline nature of XOS-3 with predominant xylose, xylobiose, xylotriose, and xyloetraose components and

their specific functional groups. It indicated the intrinsic relationship between their molecular structure and biological activity. While, XOS-3 exhibited excellent antioxidative capacities with quantifiable scavenging activities, displaying its strong antioxidant potential in biomedical applications.

The anti-osteoarthritic activity of XOS-3, particularly its role in improving cell viability and regulating markers of cartilage homeostasis was also elucidated. It provides promising insights for its therapeutic applications. These findings not only help us understand the biological activities of marine-derived polysaccharides but also highlight the therapeutic potential of XOS-3 in treating oxidative stress-related diseases and osteoarthritis.

In short, XOS-3 have been displayed a variety of functional biological activities including anti-inflammation, antioxidative, antitumor, and antimicrobial properties. These properties make it a potential candidate for functional oligosaccharides, prebiotics, and new drugs. Future research will hope to explore the mechanisms by which XOS-3 exerts its biological effects and then generate novel therapeutic strategies. The promising results of this study promote further exploration of marine polysaccharides and XOS, followed by developing new treatments for a range of medical conditions to expand the scope of carbohydrate-based therapies.

Acknowledgements

Not applicable.

Author contributions

Lixi Cai: Designed the experiment, wrote and edited the manuscript; Jinlin Zheng: Helped with experimental analysis; Lixing Liu: Performed cell experiment. Xiaoping Chen: Purified the enzyme and performed the antioxidative test; Honglin Wang: Reviewed and edited manuscript. All authors read and approved the final manuscript.

Funding

This work was funded by the Natural Science Foundation of Fujian Province of China (2021J011110), the Foundation of Fujian Educational Committee for Young and Middle-aged Teachers (JAT200496), and the Scientific Research Start-up Project of Putian University (2021071).

Availability of data and materials

The datasets used and/or analyzed during the current study are available from the corresponding author on reasonable request.

Declarations

Ethics approval and consent to participate

The experimental protocol for animal studies was reviewed and approved by the ethical review committee of Putian University [2021(07)].

Competing interests

There are no conflicts of interest or competing interests.

Author details

¹College of Basic Medicine, Putian University, Putian 351100, Fujian, People's Republic of China. ²Department of Orthopedic Surgery, Dazu Hospital of Chongqing Medical University, Chongqing 402360, People's Republic

of China. ³Putian University Key Laboratory of Translational Tumor Medicine in Fujian Province, Putian 351100, Fujian, People's Republic of China.

Received: 4 March 2024 Accepted: 7 April 2024

Published online: 16 April 2024

References

- Sun HN, Yu CM, Fu HH, Wang P, Fang ZG, Zhang YZ, Zhao F. Diversity of marine 1,3-xylan-utilizing bacteria and characters of their extracellular 1,3-xylanases. *Front Microbiol.* 2021. <https://doi.org/10.3389/fmicb.2021.721422>.
- Liu T, Yi ZW, Zeng RY, Jiang W, Zhang G. The first characterization of a Ca²⁺-dependent carbohydrate-binding module of β -1,3-xylanase from *Flammeovirga pacifica*. *Enzyme Microb Tech.* 2019. <https://doi.org/10.1016/j.enzmictec.2019.109418>.
- Kobayashi K, Kimura S, Heux L, Wada M. Crystal transition between hydrate and anhydrous (1 \rightarrow 3)- β -D-xylan from *Penicillium dumetosus*. *Carbohydr Polym.* 2013. <https://doi.org/10.1016/j.carbpol.2013.04.035>.
- Okazaki F, Nakashima N, Ogino C, Tamaru Y, Kondo A. Biochemical characterization of a thermostable β -1,3-xylanase from the hyperthermophilic eubacterium, *Thermotoga neapolitana* strain DSM 4359. *Appl Microbiol Biot.* 2013. <https://doi.org/10.1007/s00253-012-4555-5>.
- Sun Y, Gong G, Guo Y, Wang Z, Song S, Zhu B, Jiang J. Purification, structural features and immunostimulatory activity of novel polysaccharides from *Caulerpa lentillifera*. *Int J Biol Macromol.* 2018. <https://doi.org/10.1016/j.ijbiomac.2017.12.016>.
- Yuan D, Li C, Huang Q, Fu X, Dong H. Current advances in the anti-inflammatory effects and mechanisms of natural polysaccharides. *Crit Rev Food Sci.* 2023. <https://doi.org/10.1080/10408398.2022.2025535>.
- Ji X, Guo J, Tian J, Ma K, Liu Y. Research progress on degradation methods and product properties of plant polysaccharides. *J Light Ind.* 2023. <https://doi.org/10.12187/2023.03.007>.
- Palaniappan A, Antony U, Emmambux MN. Current status of xylooligosaccharides: production, characterization, health benefits and food application. *Trends Food Sci Tech.* 2021. <https://doi.org/10.1016/J.TIFS.2021.02.047>.
- Qeshmi FI, Homaei A, Fernandes P, Hemmati R, Dijkstra BW, Khajeh K. Xylanases from marine microorganisms: a brief overview on scope, sources, features and potential applications. *BBA-Proteins Proteom.* 2020. <https://doi.org/10.1016/j.bbapap.2019.140312>.
- Umemoto Y, Shibata T, Araki T. D-xylose isomerase from a marine bacterium, *Vibrio* sp. strain XY-214, and D-xylose production from β -1,3-xylan. *Mar Biotechnol.* 2012. <https://doi.org/10.1007/s10126-011-9380-9>.
- Montingelli ME, Tedesco S, Olabi AG. Biogas production from algal biomass: A review. *Renew Sust Energ Rev.* 2015. <https://doi.org/10.1016/j.rser.2014.11.052>.
- Kudou M, Okazaki F, Asai-Nakashima N, Ogino C, Kondo A. Expression of cold-adapted β -1,3-xylanase as a fusion protein with a ProS2 tag and purification using immobilized metal affinity chromatography with a high concentration of ArgHCl. *Biotechnol Lett.* 2015. <https://doi.org/10.1007/s10529-014-1666-3>.
- Cao L, Zhang R, Zhou J, Huang Z. Biotechnological aspects of salt-tolerant xylanases: a review. *J Agr Food Chem.* 2021. <https://doi.org/10.1021/acs.jafc.1c03192>.
- Zeng B, Zhao S, Zhou R, Zhou Y, Jin W, Yi Z, Zhang G. Engineering and screening of novel β -1,3-xylanases with desired hydrolysate type by optimized ancestor sequence reconstruction and data mining. *Comput Struct Biotec.* 2022. <https://doi.org/10.1016/j.csbj.2022.06.050>.
- Liang WS, Liu TC, Chang CJ, Pan CL. Bioactivity of β -1,3-xylan extracted from *Caulerpa lentillifera* by using *Escherichia coli* BL21 (DE3)- β -1,3-xylanase XYLII. *J Food Nutr Res-Slov.* 2015. <https://doi.org/10.12691/jfnr-3-7-5>.
- Maeda R, Ida T, Ihara H, Sakamoto T. Induction of apoptosis in MCF-7 cells by β -1,3-xylooligosaccharides prepared from *Caulerpa lentillifera*. *Biosci Biotech Biochem.* 2012. <https://doi.org/10.1271/bbb.120016>.
- Franková L, Fry SC. Phylogenetic variation in glycosidases and glycanases acting on plant cell wall polysaccharides, and the detection of transglycosidase and trans- β -xylanase activities. *Plant J.* 2011. <https://doi.org/10.1111/j.1365-313X.2011.04625.x>.
- Chen Y, Xie Y, Ajuwon KM, Zhong R, Li T, Chen L, Everaert N. Xylo-oligosaccharides, preparation and application to human and animal health: a review. *Front Nutr.* 2021. <https://doi.org/10.3389/fnut.2021.731930>.
- Batsalova T, Georgiev Y, Moten D, Teneva I, Dzhambazov B. Natural xylooligosaccharides exert antitumor activity via modulation of cellular antioxidant state and TLR4. *Int J Mol Sci.* 2022. <https://doi.org/10.3390/ijms231810430>.
- Zeng B, Zhou Y, Yi Z, Zhou R, Jin W, Zhang G. Highly thermostable and promiscuous β -1,3-xylanases designed by optimized ancestral sequence reconstruction. *Bioresource Technol.* 2021. <https://doi.org/10.1016/j.biortech.2021.125732>.
- Cai L, Liu X, Qiu Y, Liu M, Zhang G. Enzymatic degradation of algal 1,3-xylan: from synergism of lytic polysaccharide monoxygenases with β -1,3-xylanases to their intelligent immobilization on biomimetic silica nanoparticles. *Appl Microbiol Biot.* 2020. <https://doi.org/10.1007/s00253-020-10624-w>.
- Cai L, Gao Y, Chu Y, Lin Y, Liu L, Zhang G. Green synthesis of silica-coated magnetic nanocarriers for simultaneous purification-immobilization of β -1,3-xylanase. *Int J Biol Macromol.* 2023. <https://doi.org/10.1016/j.ijbiomac.2023.123223>.
- Shao R, Suo J, Zhang Z, Kong M, Ma Y, Wen Y, Zou W. H3K36 methyltransferase NSD1 protects against osteoarthritis through regulating chondrocyte differentiation and cartilage homeostasis. *Cell Death Differ.* 2024. <https://doi.org/10.1038/s41418-023-01244-8>.
- Ye J, Deng R, Wang X, Song S, Xu X, Zhang JY, Yu JK. Intra-articular histone deacetylase inhibitor microcarrier delivery to reduce osteoarthritis. *Nano Lett.* 2023. <https://doi.org/10.1021/acs.nanolett.3c03037>.
- Lou C, Jiang H, Lin Z, Xia T, Wang W, Lin C, Xue X. MiR-146b-5p enriched bioinspired exosomes derived from fucoidan-directed induction mesenchymal stem cells protect chondrocytes in osteoarthritis by targeting TRAF6. *J Nanobiotechnol.* 2023. <https://doi.org/10.1186/s12951-023-02264-9>.
- Zhou T, Xiong H, Yao SY, Wang S, Li S, Chang J, Gao C. Hypoxia and matrix metalloproteinase 13-responsive hydrogel microspheres alleviate osteoarthritis progression in vivo. *Small.* 2023. <https://doi.org/10.1002/sml.202308599>.
- Wei G, Lu K, Umar M, Zhu Z, Lu WW, Speakman JR, Chen D. Risk of metabolic abnormalities in osteoarthritis: a new perspective to understand its pathological mechanisms. *Bone Res.* 2023. <https://doi.org/10.1038/s41413-023-00301-9>.
- Kang MG, Lee HJ, Cho JY, Kim K, Yang SJ, Kim D. Anti-inflammatory effects of sucrose-derived oligosaccharides produced by a constitutive mutant L mesenteroides B-512FMC dextranase in high fat diet-fed mice. *Biochem Biophys Res Commun.* 2016. <https://doi.org/10.1177/1947603517749919>.
- Kang Z, Zhou Z, Wang Y, Huang H, Du G, Chen J. Bio-based strategies for producing glycosaminoglycans and their oligosaccharides. *Trends Biotechnol.* 2018. <https://doi.org/10.1016/j.tibtech.2018.03.010>.
- Zhang C, Yu L, Zhou Y, Zhao Q, Liu SQ. Chitosan oligosaccharides inhibit IL-1 β -induced chondrocyte apoptosis via the P38 MAPK signaling pathway. *Glycoconj J.* 2016. <https://doi.org/10.1007/s10719-016-9667-1>.
- Einarsson JM, Bahrke S, Sigurdsson BT, Ng CH, Petersen PH, Sigurjonsson OE, Jonsson H. Partially acetylated chitoooligosaccharides bind to YKL-40 and stimulate growth of human osteoarthritic chondrocytes. *Biochem Biophys Res Commun.* 2013. <https://doi.org/10.1016/j.bbrc.2013.02.122>.
- Yu C, Zang H, Yang C, Liang D, Quan S, Li D, Li Y, Dong Q, Wang F, Li L. Study of chondroitin sulfate E oligosaccharide as a promising complement C5 inhibitor for osteoarthritis alleviation. *Mater Sci Eng C Mater Biol Appl.* 2021. <https://doi.org/10.1016/j.msec.2021.112234434:298-304>.
- Zhang C, Liao Q, Ming JH, Hu GL, Chen Q, Liu SQ, Li YM. The effects of chitosan oligosaccharides on OPG and RANKL expression in a rat osteoarthritis model. *Acta Cir Bras.* 2017. <https://doi.org/10.1590/s0102-86500170060000002>.
- Cai L, Chu Y, Liu X, Qiu Y, Ge Z, Zhang G. A novel all-in-one strategy for purification and immobilization of β -1,3-xylanase directly from cell lysate as active and recyclable nanobiocatalyst. *Microb Cell Fact.* 2021. <https://doi.org/10.1186/s12934-021-01530-5>.
- Iriki Y, Suzuki T, Nisizawa K, Miwa T. Xylan of siphonaceous green algae. *Nature.* 1960. <https://doi.org/10.1038/187082a0>.

36. Ji X, Guo J, Ding D, Gao J, Hao L, Guo X, Liu Y. Structural characterization and antioxidant activity of a novel high-molecular-weight polysaccharide from *Ziziphus Jujuba* cv. Muzao J Food Meas Charac. 2022. <https://doi.org/10.1007/s11694-022-01288-3>.
37. Zhang M, Zhao M, Qing Y, Luo Y, Xia G, Li Y. Study on immunostimulatory activity and extraction process optimization of polysaccharides from *Caulerpa lentillifera*. Int J Biol Macromol. 2020. <https://doi.org/10.1016/j.ijbiomac.2019.10.042>.
38. Sonkar RM, Gade PS, Mudliar SN, Bhatt P. Green downstream processing method for xylooligosaccharide purification and assessment of its prebiotic properties. ACS Omega. 2023. <https://doi.org/10.1021/acsomega.3c05714>.
39. Santibáñez L, Henríquez C, Corro-Tejeda R, Bernal S, Armijo B, Salazar O. Xylooligosaccharides from lignocellulosic biomass: a comprehensive review. Carbohydr Polym. 2021. <https://doi.org/10.1016/j.carbpol.2020.117118>.
40. Henriques PI, Serrano MDLS, de Sousa APM, Alves AMFB. Green process for xylooligosaccharides production using an *Eucalyptus Kraft* Pulp. J Polym Environ. 2023. <https://doi.org/10.1007/s10924-022-02728-3>.
41. Hou C, Yin M, Lan P, Wang H, Nie H, Ji X. Recent progress in the research of *Angelica sinensis* (Oliv.) Diels polysaccharides: extraction, purification, structure and bioactivities. Chem Biol Technol Ag. 2021. <https://doi.org/10.1186/s40538-021-00214-x>.
42. Wang L, Zhang Z, Zhao W, Lin C, Zhou X, Pang H, Ma B. Physicochemical, rheological, antioxidant and immunological properties of four novel non-inulin (poly)saccharides from *Asparagus cochinchinensis*. Int J Biol Macromol. 2024. <https://doi.org/10.1016/j.ijbiomac.2023.129034>.
43. Ji X, Cheng Y, Tian J, Zhang S, Jing Y, Shi M. Structural characterization of polysaccharide from jujube (*Ziziphus jujuba* Mill.) fruit. Chem Biol Technol Agric. 2021. <https://doi.org/10.1186/s40538-021-00255-2>.
44. Zhan K, Ji X, Luo L. Recent progress in research on *Momordica charantia* polysaccharides: extraction, purification, structural characteristics and bioactivities. Chem Biol Technol Agric. 2023. <https://doi.org/10.1186/s40538-023-00433-4>.
45. Yarley OPN, Kojo AB, Zhou C, Yu X, Gideon A, Kwadwo HH, Richard O. Reviews on mechanisms of in vitro antioxidant, antibacterial and anticancer activities of water-soluble plant polysaccharides. Int J Biol Macromol. 2021. <https://doi.org/10.1016/j.ijbiomac.2021.05.181>.
46. Valls C, Pastor FJJ, Vidal T, Roncero MB, Díaz P, Martínez J, Valenzuela SV. Antioxidant activity of xylooligosaccharides produced from glucuronoxylan by Xyn10A and Xyn30D xylanases and eucalyptus autohydrolysates. Carbohydr Polym. 2018. <https://doi.org/10.1016/j.carbpol.2018.04.028>.
47. Xue CH, Fang Y, Lin H, Chen L, Li ZJ, Deng D, Lu CX. Chemical characters and antioxidative properties of sulfated polysaccharides from *Laminaria japonica*. J Appl Phycol. 2001. <https://doi.org/10.1023/A:1008103611522>.
48. Ji X, Guo J, Cao T, Zhang TK, Liu Y, Yan Y. Review on mechanisms and structure-activity relationship of hypoglycemic effects of polysaccharides from natural resources. Food Sci Hum Well. 2023. <https://doi.org/10.1016/j.fshw.2023.03.017>.
49. Yuan Q, Yuan Y, Zheng Y, Sheng R, Liu L, Xie F. Anti-cerebral ischemia reperfusion injury of polysaccharides: a review of the mechanisms. Biomed Pharmacother. 2021. <https://doi.org/10.1016/j.biopha.2021.111303>.
50. Taku S, Atsushi F, Akihiko M, Toshiyuki I, Fumiko Y, Shinsuke O. Transcriptional regulation of endochondral ossification by HIF-2 α during skeletal growth and osteoarthritis development. Nat Med. 2010. <https://doi.org/10.1038/nm.2146>.
51. Yamani L, Kristanti A, Puspaningsih N. The preliminary study of antioxidant activity from xylo-oligosaccharide of corncob (zea mays) hydrolysis product with endo- β -xylanase enzyme. J Infect Dis. 2016. <https://doi.org/10.20473/JTID.V3I2.219>.
52. Erfan AE, Ming L, Patricia EH, Jules D, Glynn M, Andrew F. Overexpression of MMP13 in human osteoarthritic cartilage is associated with the SMAD-independent TGF- β signalling pathway. Arthritis Res Ther. 2015. <https://doi.org/10.1186/s13075-015-0788-x>.

Publisher's Note

Springer Nature remains neutral with regard to jurisdictional claims in published maps and institutional affiliations.